2010 IEEE International Conference on Robotics and Automation
Anchorage Convention District
May 3-8, 2010, Anchorage, Alaska, USA

A Hybrid Estimation Approach for Autonomous Dirt Road Following using Multiple Clothoid Segments

Michael Manz, Felix von Hundelshausen and Hans-Joachim Wuensche

***Abstract*— In this paper we describe a novel approach to autonomous dirt road following. The algorithm is able to recognize highly curved roads in cluttered color images quite often appearing in offroad scenarios. To cope with large curvatures we apply gaze control and model the road using two different clothoid segments. A Particle Filter incorporating edge and color intensity information is used to simultaneously detect and track the road farther away from the ego vehicle. In addition the particles are used to generate static road segment estimations in a given look ahead distance. These estimations are predicted with respect to ego motion and fused utilizing Kalman filter techniques to generate a smooth local clothoid segment for lateral control of the vehicle.**

I. Introduction

Visual road recognition has a long research history and is one of the key capabilities needed by autonomous vehicles. For this reason numerous autonomous road following systems have been developed worldwide by different groups, using many different image features and tracking algorithms [1]. Even more than ten years ago road following algorithms like GOLD (General Obstacle and Lane Detection) [2], RALPH (Rapidly Adapting Lateral Position Handler) [3], SCARF (Supervised Classification Applied to Road Following) [4], YARF (Yet Another Road Follower) [5], LOIS (Likelihood Of Image Shape) [6] and EMS-Vision (Expectation-based Multi-focal Saccadic Vision) [7] showed impressive results. Although all of them proved their strength in difficult road scenarios, they all have some kind of weakness.

For instance, Luetzeler [8] developed an algorithm based on the well known EMS-Vision system which enabled a tracked vehicle to autonomously drive up to 50 km/h on a dirt road. However, errors arose if the road boundary edges were of low contrast or heavily cluttered.

In order to develop more robust road tracking algorithms and with the enhancement of computational power, particle filters [9] have gained more and more interest within the area of road recognition in recent years. They are able to cope with heavily cluttered image data within the estimation scheme and to reduce the image processing complexity to a rating of particular hypotheses. Furthermore particle filters ease the fusion of different road features which further increase the robustness of the overall estimator.

A first approach using a particle filter framework for road recognition was presented by Southall [10], who used a clothoid model and extracted road markings on highway road scenes to estimate the location of the road relative to the vehicle. Since then several particle filter based road trackers have been proposed. Apostoloff and Zelinsky [11] developed the so called *distillation algorithm* which combines a particle filter with a cue fusion engine to track marked roads, fusing edge, color and road marking information. To detect marked roads up to 100m during night time driving, Smuda et al. [12] fused texture, edge and map information. Further work extended the use of particle filter based methods to country roads using some combination of edge, color and intensity information [13] and improved the lane recognition capabilities during night time driving utilizing a digital map as well as image gradient information and an imaging radar system [14]. In order to improve the robustness of road tracking in difficult road scenarios Danescu et al. [15] fused edge and lane marking information with 3D cues gathered by a stereo vision system. Recently, Lose et al. [16] further improved the estimation quality on country roads by fusing stereo and edge information using a Kalman particle filter.

Summarizing, a lot of problems have been solved since the introduction of particle filters within the area of road recognition. However, all of the mentioned particle filter based road tracking algorithms have one common limitation. They all work with a single road segment and use image features extracted some meters in front of the vehicle to estimate the road location relative to the vehicle center. Thus problems arise in highly curved roads as a single clothoid segment can not always accurately model the road within a given look ahead distance (see figure 1(b)). This can lead to faulty estimations of the road location with reference to the vehicle center of gravity and thus to bad road following behavior. Using map information (e.g. as in [12], [14]) can partly solve this problem but accurate maps and an adequate localization in the map are often not available, especially in offroad scenarios. In addition the mentioned particle filter

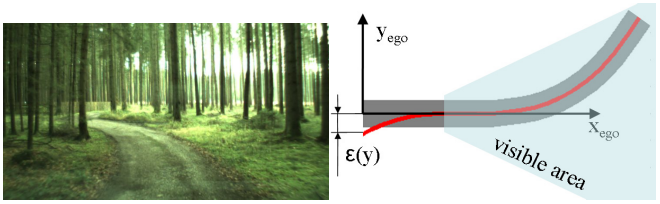

(a) (b)

Fig. 1. (a) typical color image of a dirt road (b) displacement error $\epsilon(y)$ at the vehicle center occurring even by an optimal fit of a single clothoid segment (red line) on a road (gray) within the visible area

All authors are with the Institute for Autonomous Systems Technology (TAS), University of the Bundeswehr Munich, 85577 Neubiberg, Germany. Contact author email: michael.manz@unibw.de

based road tracking algorithms are not designed to cope with dirt road scenarios. A color image of a typical dirt road in a forest scene can be seen in figure 1(a).

In order to overcome the model limitations of a single clothoid segment and simultaneously be able to detect, track and autonomously follow highly horizontal curved dirt roads we introduce a three-stage tracking algorithm utilizing two clothoid segments and two different filter techniques.

Section II describes the first stage of the algorithm where a particle filter fusing three different image cues is utilized to detect and track a dirt road several meters ahead of the vehicle.

In the second stage (see Section III), the particles of the filter are used to provide short static road segment estimations relative to the ego vehicle. These static segments are then predicted wrt. ego motion to produce a chain of static road segments. A somewhat similar idea was proposed by Kluge and Thorpe within the YARF [5] system. They accumulate image measurement from multiple images within a local map to produce dense road edge measurements next to the vehicle.

The third stage of the algorithm, explained in section IV, fuses the predicted static road segments in the vicinity of the vehicle using an Extended Kalman Filter (EKF) to generate a smooth clothoidal road segment estimation for the lateral control unit, even in highly curved roads. The last two stages can be seen as an enhancement and an adaption of our vehicle following approach presented in [17] to the problem of autonomous road following.

Some experimental results are presented in section V.

II. Road Recognition

In order to detect and track the dirt road within the color image we utilize the 4D-approach [18]. We model the 3D geometry of the road as well as the vehicle and road curvature dynamics and use a particle filter framework to recursively estimate the road geometry and position relative to the vehicle's center. To rate a particle i and the road hypothesis $\mathbf{x}_{pf}^{(i)}$ it represents, we fuse color saturation information with color gradient measures. In order to enable the tracker to recover from any loss of lock that may occur, we introduce in each time step a small percentage of initialization particles drawn from a distribution of reasonable road hypotheses. Camera gaze direction is controlled in order to keep the mean road position in a given look ahead distance within the visible area of the camera, even in sharp turns.

A. Road Model

The road model used within the particle filter is a clothoid segment with start curvature $c_{0_{pf}}$, change of curvature $c_{1_{pf}}$ and road width w_{pf}. [1] The start point x_{pf}, y_{pf} of the segment is defined to have a constant distance to the ego coordinate system center r_{cam} (see figure 2). To allow a good fit even for highly curved roads we do not, like other approaches (e.g. [8], [13]), approximate the clothoid equations by a polygon

[1]Here the subscript 'pf' indicates that the values are estimated with the proposed particle filter (far range road estimation, first algorithm stage)

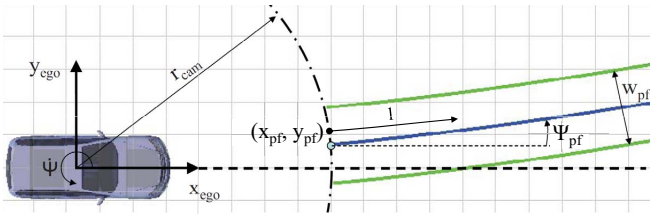

Fig. 2. Road model used within the particle filter

of order three, but use the exact clothoid equations to get the road azimuth angle χ_{road},

$$\chi_{road}(l) = \Psi_{pf} + \left(c_{0_{pf}} + \frac{c_{1_{pf}} l}{2}\right) l \tag{1}$$

where l is a control variable along the clothoid arc length and Ψ_{pf} is the road yaw angle at the start position of the road model. The coordinates $x_{road}(l), y_{road}(l)$ of the clothoid segment result from the integration of the road azimuth angle over the segment arc length and can be approximated by the sum

$$x_{road}(l_j) \approx x_{pf} + \sum_{i=0}^{j} cos(\chi_{road}(l_i))\Delta l \tag{2}$$

$$y_{road}(l_j) \approx y_{pf} + \sum_{i=0}^{j} sin(\chi_{road}(l_i))\Delta l \tag{3}$$

where l_j and l_i are arc length samples with distance Δl along the clothoid segment.

To get a representation of the road model within the image coordinate system we project all road points $x_{road}(l_j), y_{road}(l_j)$ onto the image plane, incorporating information from the calibrated camera system as well as gaze direction and measurements of an on board IMU.

B. Dynamic Model

The road is modeled as a static object. However, as the vehicle moves, the road's position changes according to inverse ego motion. Given the road's state vector at time index k,

$$\mathbf{x}_{pf_k} = [x_{pf}, y_{pf}, \Psi_{pf}, c_{0_{pf}}, c_{1_{pf}}, w_{pf}]^T \tag{4}$$

the first temporal transition of the state vector can be calculated by

$$\mathbf{x}^{*-}_{pf_{k+1}} = \mathbf{\Phi}_{pf_k}\hat{\mathbf{x}}_{pf_k} + \begin{pmatrix} -cos(\dot{\Psi}\Delta t - \beta)v\Delta t \\ sin(\dot{\Psi}\Delta t - \beta)v\Delta t \\ -\dot{\Psi}\Delta t \\ \mathbf{0}_{3\times 1} \end{pmatrix} + \mathbf{w}_{pf_k} \tag{5}$$

where Δt is the time between two successive images, v represents vehicle velocity and β is the slip angle of the vehicle. Given the yaw rate $\dot{\Psi}$ of the vehicle we can derive the discrete transition matrix $\mathbf{\Phi}_{pf_k}$:

$$\mathbf{\Phi}_{pf_k} = \begin{pmatrix} \mathbf{R}_{z_k} & \mathbf{0} \\ \mathbf{0} & \mathbf{I}_{4\times 4} \end{pmatrix}; \mathbf{R}_{z_k} = \begin{pmatrix} cos(\dot{\Psi}\Delta t) & sin(\dot{\Psi}\Delta t) \\ -sin(\dot{\Psi}\Delta t) & cos(\dot{\Psi}\Delta t) \end{pmatrix} \tag{6}$$

All ego motion parameters ($\dot{\Psi}$, β, v) are provided by an on-line ego motion estimation process based on the bicycle model for lateral vehicle dynamics using an EKF. In order to consider uncertainty within the dynamic model a Gaussian random vector $\mathbf{w}_{pf_k}$ is added to equation 5.

With the vehicle moving, successive prediction steps would cause the static road segment to leave the visual range of the used camera. Thus, after the first prediction (equation 5), we further adjust the calculated state vector $\mathbf{x}_{pf}^{*-}$ in order to maintain a constant distance (r_{cam}) of the clothoid start position (x_{pf}^*, y_{pf}^*) to the ego vehicle center. This is archieved by calculation the intersection point of the predicted clothoid with a circle of radius r_{cam}. Knowing the arc length l_p along the static clothoid segment up to the intersection point one can further predict Ψ_{pf}^{*-} and $c_{0_{pf}}^{*-}$:

$$\Psi_{pf}^* = \Psi_{pf}^{*-} + \left(c_{0_{pf}}^{*-} + \frac{c_{1_{pf}}^{*-} l_p}{2} \right) l_p \quad (7)$$

$$c_{0_{pf}}^* = c_{0_{pf}}^{*-} + c_{1_{pf}}^{*-} l_p \quad (8)$$

The road width w_{pf}^* and the change of curvature $c_{1_{pf}}^*$ are taken to be constant.

C. Measurement Model

The key point of the measurement update equation is to get the probability density function $p(\mathbf{x}_k|\mathbf{Y}_k)$ of the state $\mathbf{x}_k$ at time index k conditioned on all measurements $\mathbf{Y}_k = \mathbf{y}_1, \mathbf{y}_2, ...\mathbf{y}_k$. This can be formulated as a recursive Bayesian estimation problem

$$p(\mathbf{x}_k|\mathbf{Y}_k) \propto p(\mathbf{y}_k|\mathbf{x}_k) p(\mathbf{x}_k|\mathbf{Y}_{k-1}) \quad (9)$$

where $p(\mathbf{y}_k|\mathbf{x}_k)$ is the likelihood function of the current measurement $\mathbf{y}_k$ given $\mathbf{x}_k$.

The purpose of the likelihood function is to assign each predicted particle $\mathbf{x}_{pf_k}^{*(i)}$ a specific weight, reflecting the likelihood of the hypothesis according to all available current measurements $\mathbf{y}_k$. In our algorithm we introduce three different image based measurements (saturation $\mathbf{y}_{k_s}$, color edge intensity $\mathbf{y}_{k_I}$ and color edge direction $\mathbf{y}_{k_d}$) and one heuristic cue based on the overall knowledge of the road width $\mathbf{y}_{k_w}$. Thus $\mathbf{y}_k$ has four components and we have to evaluate the joint probability $p(\mathbf{y}_{k_s}, \mathbf{y}_{k_I}, \mathbf{y}_{k_d}, \mathbf{y}_{k_w}|\mathbf{x}_{pf_k}^{*(i)})$. Using the sum rule of probability, this joint probability factors into,

$$\begin{aligned} p(\mathbf{y}_{k_s}, \mathbf{y}_{k_I}, \mathbf{y}_{k_d}, \mathbf{y}_{k_w}|\mathbf{x}_{pf_k}^{*(i)}) &= p(\mathbf{y}_{k_I}|\mathbf{x}_{pf_k}^{*(i)}) p(\mathbf{y}_{k_d}|\mathbf{x}_{pf_k}^{*(i)}, \mathbf{y}_{k_I}) \\ & \quad p(\mathbf{y}_{k_s}|\mathbf{x}_{pf_k}^{*(i)}) p(\mathbf{y}_{k_w}|\mathbf{x}_{pf_k}^{*(i)}) \quad (10) \end{aligned}$$

where we do not, like several other approaches (e.g. [16], [13]), treat the measurements as statistically independent from each other, but introduce one additional conditional dependency $p(\mathbf{y}_{k_d}|\mathbf{x}_{pf_k}^{*(i)}, \mathbf{y}_{k_I})$, i.e. we state that the likelihood of the color edge given $\mathbf{x}_{pf_k}^{*(i)}$ depends on the edge gradient intensity. We discuss this in more detail in II-C.3. After the description of the cue fusion concept we now specify the single likelihood functions.

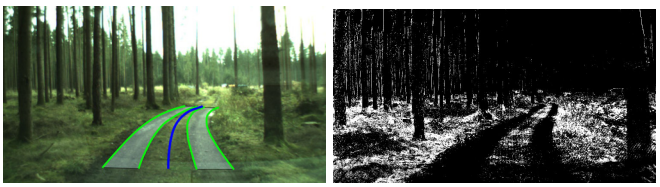

(a) (b)

Fig. 3. (a) Color image of a dirt road scene with projected road model (blue line is the road skeleton line, outer green lines are the road boundaries $RB^{(i)}$, light blue area reflect the support road area for the saturation feature $RA^{(i)}$). (b) Weighted image due to transformation function for the saturation channel (bright pixels encode non-road areas)

1) Saturation: As proposed in [19] we utilize the saturation channel of the HSI color space to efficiently segment non-road pixels in dirt road images. The feature makes use of the knowledge we gained in numerous experiments – that the road surface may show all kinds of colors but there will be only a vanishing amount of brightly colored pixels on a road's surface. In the opposite, this means that almost all brightly colored image areas will most likely correspond to non-road areas. This is especially true on dirt road where the road is typically surrounded by some kind of vegetation.

To further enhance this effect we weight the value of each saturation pixel $s(y,z)$ according to the dynamic function,

$$I_s(y,z) = \begin{cases} 0, & s(y,z) \leq \mu_s \\ \frac{255(s(y,z)-\mu_s)}{s_{off}}, & \mu_s < s(y,z) < (\mu_s + s_{off}) \\ 255, & s(y,z) \geq (\mu_s + s_{off}) \end{cases} \quad (11)$$

where μ_s represents the temporally low-pass filtered mean saturation value in the lower image parts and s_{off} is a parameter to adapt the weighting transition. To speed up the process we use look up tables to evaluate equation (11). An exemplary segmentation result obtained by applying this saturation feature to real data is shown in figure 3(b).

To get a weighting function representing the likelihood $p(\mathbf{y}_{k_s}|\mathbf{x}_{pf_k}^{*(i)})$ of a particle i needed in the cue fusion concept, we use the sum of all weighted saturation values $I_s(y,z)$ corresponding to the projected support area $RA^{(i)}$ (see the two bands in figure 3(a)) defined by the particle $\mathbf{x}_{pf_k}^{*(i)}$,

$$p(\mathbf{y}_{k_s}|\mathbf{x}_{pf_k}^{*(i)}) = \frac{1}{z_s} e^{-\frac{1}{2\sigma_s^2} \left(\frac{1}{N_{RA}^{(i)}} \sum_{(y,z) \in RA^{(i)}} I_s(y,z) \right)^2} \quad (12)$$

where $N_{RA}^{(i)}$ is the number of all road area pixels, z_s is a normalizing constant and σ_s^2 is the saturation features predefined variance.

2) Color Edge Intensity: One of the most important image cues concerning road recognition, used in many former lane tracking systems as the main feature (e.g. [7], [2]), is the rise in image gradient intensities near road borders. Even in dirt road scenarios where image edges are severely cluttered, it is still advantageous to use image gradient information. In order to evaluate the image gradients we correlate each channel of the RGB-intensity images in horizontal and vertical direction

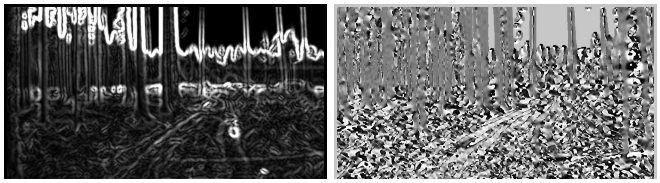

(a) (b)

Fig. 4. (a) gradient intensity of a dirt road image (b) intensity encoded image of the gradient phase

with a large ternary correlation mask similar to [7], resulting in heavily low pass filtered gradient images. Out of these, the overall color intensity gradient image I_I is set to be the maximum norm of the normalized gradients computed for each color channel (see figure 4(a)).

To get a weighting function representing the likelihood $p(\mathbf{y}_{k_I}|\mathbf{x}^{*(i)}_{pf_k})$ of a particle i needed in the cue fusion concept, we use the sum of gradient intensity values $I_I(y,z)$ corresponding to the projected road boundaries $RB^{(i)}$ (see figure 3(a)) defined by each $\mathbf{x}^{*(i)}_{pf_k}$,

$$p(\mathbf{y}_{k_I}|\mathbf{x}^{*(i)}_{pf_k}) = \frac{1}{z_I}\left(\frac{1}{N^i_{RB}}\sum_{(y,z)\in RB^{(i)}} I_I(y,z)\right)^n \tag{13}$$

where N^i_{RB} is the number of all road boundary pixels, z_I is a normalizing constant and $n > 1$ can be used to emphasize hypotheses with strong road boundary gradients.

3) Color Edge Direction: The overall phase of the RGB-gradient $I_d(y,z)$ is set to be the direction of the strongest gradient found in II-C.2. As can be seen in figure 4(b) the gradient phase is a heavily cluttered measurement and can not be accurately determined for low image gradients, i.e. the stronger the gradient intensity the higher the meaningfulness of the phase information. Thus, we have to evaluate the likelihood of the measurement $\mathbf{y}_{k_d}$ given both the particle $\mathbf{x}^{*(i)}_{pf_k}$ and the gradient intensity measure $\mathbf{y}_{k_I}$. We do so with the aid of a weighted mean of the difference between the expected phase $d^{(i)}(y,z)$ gained from the i-th particle and the gradient phase $I_d(y,z)$ along the hypothetical road boundary $RB^{(i)}$,

$$p(\mathbf{y}_{k_d}|\mathbf{x}^{*(i)}_{pf_k}, y_{k_I}) = \frac{1}{z_d}e^{-\frac{1}{2\sigma_d^2}\frac{\sum_{(y,z)\in RB^{(i)}}(I_d(y,z)-d^{(i)}(y,z))^2 I_I(y,z)}{\sum_{(y,z)\in RB^{(i)}} I_I(y,z)}} \tag{14}$$

where z_d is a normalization constant and σ_d^2 is a predefined variance of the phase measurement.

4) Heuristic Road Width: In order to keep the particles in a meaningful state space region based on prior knowledge of the mean dirt road width W and width variance σ_w^2, we incorporate a fourth particle likelihood function $p(\mathbf{y}_{k_w}|\mathbf{x}^{*(i)}_{pf_k})$ into the estimation process. This function is based on the likelihood of correspondence of the current particle road width $w^{*(i)}_{pf}$ given a predefined Gaussian distribution $N(W,\sigma_w^2)$ (see [11]).

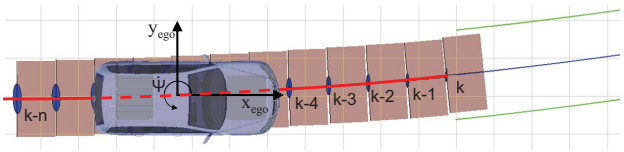

Fig. 5. Generation of successive static road segments (brown areas) with predicted error covariances (blue ellipses) and estimation of the local clothoid segment (red line)

III. Static Road Segments

We define a static road segment to be a small fraction of the road with specific length L_{rs}. The segment can be described by a state vector $\mathbf{x}(t)_{rs} = [x_{rs}, y_{rs}, \Psi_{rs}]$ where x_{rs}, y_{rs} are the x and y coordinates within the ego-coordinate system and Ψ_{rs} is the yaw angle of the road segment relative to the vehicle's longitudinal axis. In the proposed algorithm, static road segments are successively generated and later used to estimate a second clothoid segment more closer to the vehicle (Section IV)

A. Generation of Road Segments

In order to generate successive static road segments (see figure 5) we use the 50 best particles gained from the particle filter estimation of the first clothoid segment and calculate their mean $\hat{\mathbf{x}}_{pf}$ and their error-covariance $\hat{\mathbf{P}}_{pf}$.

To get the start error-covariance $\hat{\mathbf{P}}_{rs}$ and mean state vector $\hat{\mathbf{x}}_{rs}$ of the static road segment only the first three states of the particle filter estimate $\hat{\mathbf{x}}_{pf}$, which are equal to the state vector of a single static road segment $\mathbf{x}_{rs}$, are considered. In order to get a good spreading of the generated road segments, resulting in a better clothoid estimation in the next section IV, new static road segments are only generated if the ego vehicle has approximately driven a distance L_{rs} since the generation of the last static road segment.

B. Prediction of Road Segments

Figure 5 pictures the prediction of successively generated segments used to generate a chain of small sized local road segments. The deterministic part of the prediction $\mathbf{x}^*_{rs_{k+1}} = f(\hat{\mathbf{x}}_{rs_k}, \Psi, \beta, v, \Delta t)$ is given by the first temporal transition equations of the first three states of the particle filter estimation in section II-B (equation 5). To predict the uncertainty of a road segment we use the UDU-factorized form of the standard Kalman filter prediction equation,

$$\mathbf{P}^*_{rs_{k+1}} = \mathbf{\Phi}_{pfsub_k}\hat{\mathbf{P}}_{rs_k}\mathbf{\Phi}^T_{pfsub_k}(t) + \mathbf{Q}_{rs_k} \tag{15}$$

where $\mathbf{\Phi}_{pfsub}$ is again a sub matrix of $\mathbf{\Phi}_{pf}$ (see section II-B) corresponding to the states of $\mathbf{x}_{rs}$. Because the uncertainty in the ego motion parameters depend on the vehicle's current dynamic state, we choose $\mathbf{Q}_{rs_k}$ to be a time varying covariance matrix.

IV. Local Road estimation

In order to get smooth feedback quantities for the lateral control unit we utilize a UDU-factorized EKF. The filter is used to estimate the position and geometry of a local clothoid

segment based on the chain of predicted static road segments $\mathbf{x}^*_{rs}(k, ..., k-n)$ generated in the previous step (section III). Figure 5 shows an exemplary estimation result of the local clothoid segment.

A. Road Model

For the use within the EKF we stick to the standard clothoidal approximation presented in [20],

$$y_{road}(l_j) = \frac{1}{2}c_{0_{kf}}l_j^2 + \frac{1}{6}c_{1_{kf}}l_j^3\,; \quad x_{road}(l_j) = l_j \tag{16}$$

where $c_{0_{kf}}$ [1] is the curvature of the road at the vehicle center of gravity, $c_{1_{kf}}$ is the change of curvature and l_j samples over the segment length. The clothoidal road segment is placed in a specific lateral distance y_{kf} to the vehicle's longitudinal axis and is rotated according to the road yaw angle ψ_{kf}. These transformations are all performed using homogeneous transformation matrices.

B. Dynamic Model

Based on the road model description IV-A and the so called average clothoid model [18] we define the state to be estimated:

$$\mathbf{x}_{kf} = \left[y_{kf}, tan(\psi_{kf}), c_{0m_{kf}}, c_{1m_{kf}}, c_{1_{kf}}\right] \tag{17}$$

Like [10] we are using the state variable $tan(\psi_{kf})$ to account for large road yaw angles ψ_{kf} which can appear during dirt road driving. With the state vector $\mathbf{x}_{kf}$ and the variable $\Delta x = v\Delta t cos(\psi_{kf})$ we can derive the dynamic model,

$$\mathbf{x}^*_{kf_{k+1}} = \mathbf{\Phi}_{kf_k}\hat{\mathbf{x}}_{kf_k} + \begin{pmatrix} 0 \\ -\Delta t \\ 0 \\ 0 \\ 0 \end{pmatrix}\dot{\Psi} + \mathbf{w}_{kf_k} \tag{18}$$

where

$$\mathbf{\Phi}_{kf_k} = \begin{pmatrix} 1 & \Delta x & \frac{\Delta x^2}{2} & \frac{\Delta x^3}{6} & 0 \\ 0 & 1 & \Delta x & \frac{\Delta x^2}{2} & 0 \\ 0 & 0 & 1 & \frac{L_v(1-\rho)}{3} & \frac{L_v(1-\rho)}{3} + v\Delta t \\ 0 & 0 & 0 & \rho & 1-\rho \\ 0 & 0 & 0 & 0 & 1 \end{pmatrix} \tag{19}$$

and

$$\rho = \exp\left(-\frac{3v\Delta t}{L_v}\right) \tag{20}$$

Here, L_v is the length of the clothoid segment in positive x-direction and $\mathbf{w}_{kf_k}$ specifies a Gaussian random process with known covariance matrix.

C. Measurement Model

The measurement is given by the set of N static road segments $\mathbf{x}^*_{rs}(k, ..., k-n)$ (see figure 5). Because the static road segments are taken to be uncorrelated, a block wise sequential innovation step is performed. The covariance matrix $\mathbf{R}_{rs}(k-n)$ representing the uncertainty of a measurement n is set to be equal to the corresponding error covariance matrix $\mathbf{P}^*_{rs}(k-n)$ of the considered static road segment.

[1]The subscript 'kf' represents EKF estimations (third algorithm stage)

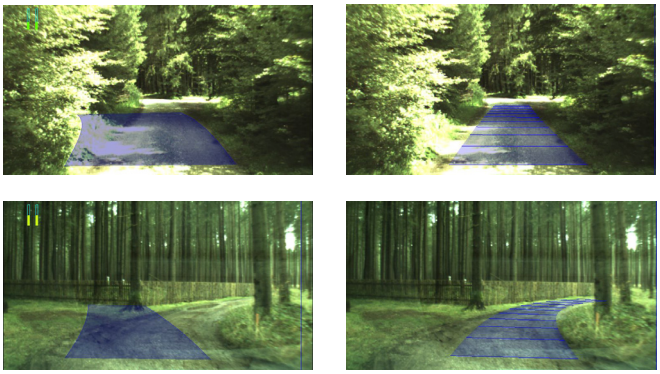

Fig. 6. On the left side common failure modes of a EKF based road tracker are shown whereas the tracking result with the proposed particle filter framework can be seen on the right

V. Experimental Results

Because the image of a dirt road is heavily cluttered and the road boundaries can not precisely be located it is beneficial for both the road detection as well as the computation time to work with a quarter of the original wide VGA image resolution. We have implemented the proposed tracking algorithm on a multi processor system (Intel Xeon L5420 Dual CPU Quad Core) on board our test vehicle MuCAR-3 (Munich Cognitive Autonomous Robot Car 3^{rd} Generation). Using two cores and 400 particles and utilizing the Intel performance primitives[2] the algorithm takes $35ms$ of CPU time. With an overall system cycle of $50ms$ it easily fulfills real time requirements.

To evaluate the robustness of the proposed road recognition method we first compared it's tracking results to those of an EKF based road tracker using only image edge informations similar to those used in [8]. Figure 6 shows common failure modes of the EKF based tracker arising because of complex shadows and weak road corners and the successful tracking of the particle filter in the same sequence.

Furthermore, the proposed particle filter for road detection has proved its robustness in several kilometers of autonomous dirt road driving at speeds up to 50 km/h limitid mainly because of rough road condition. An accompanying video file (*ICRA10_0922_VI_i.mp4*) shows autonomous driving ($v \approx 4\frac{m}{s}$) through dense wood where the algorithm has to cope with complex lighting conditions, heavily cluttered road image, crossings and curved roads. Note that varying Δt values up to $200ms$ occur caused by varying integration times of the camera sensor.

An exemplary estimation of the lateral road displacement y recorded during that autonomous drive is pictured in Figure 7. It can clearly be seen that, because of the discretization of the state space by a low number of particles, the estimated displacement gained from the particle filter y_{pf} (blue line) is noisy. But thanks to the multi stage tracking approach a really smooth estimate of the displacement at the vehicle center y_{kf} (green line) is achieved. The difference between

[2]http://software.intel.com/en-us/intel-ipp/

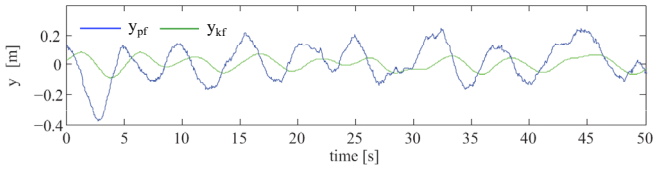

Fig. 7. Displacement gained from both clothoid segment estimations of the proposed hybrid estimation approach during autonomous driving

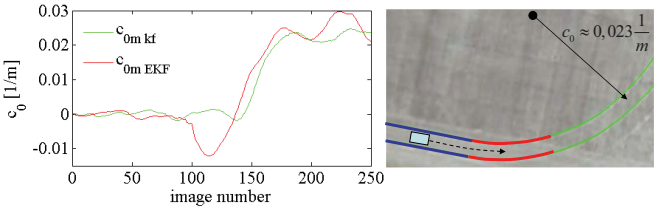

Fig. 8. Estimation of the road curvature (left) as MuCar-3 is driving through a left turn with known clothoid segments (right). Blue indicates a straight segment followed by a transition curve (red) and a circular arc (green)

amplitude and phase of both estimates is mainly because of the diverse longitudinal positions the displacements are estimated at. The low pass effect of the used EKF is marginal due to good prediction models.

In order to evaluate the abilities of the proposed tracking of two different clothoid segments we compared the estimation result of the curvature c_{0m} at the vehicles center of gravity. Figure 8 shows an estimation of the curvature obtained from the proposed multi stage tracking algorithm ($c_{0m_{kf}}$) and from a standard EKF based road tracker ($c_{0m_{EKF}}$ see [7]) using only a single segment while MuCAR-3 is driving through three marked clothoidal road segments. Within the straight segment both algorithms perform well. However, coming close to the transition curve the road course can no longer be approximated by a single road segment and thus the tracker using a single road segment estimates a erroneous horizontal curvature to the right and additionally overestimates the road curvature at the beginning of the circular arc segment. In contrast, thanks to the usage of two clothoid segments, the proposed algorithm significantly reduces such errors.

A further advantage of the proposed algorithm we discovered during test drives is, that short-term detection errors of the particle filter in curvature and curvature change do not influence autonomous road following. This is because the clothoid path generation used for lateral vehicle control only depends on the detected road position (x_{pf}, y_{pf}, $\Psi_{0_{pf}}$) but not on $c_{0_{pf}}$ and $c_{1_{pf}}$. This can significantly increase the robustness of the autonomous road following in difficult situations.

VI. Conclusion

We have presented a vision based multi stage estimation scheme utilizing a particle filter to detect and track a dirt road within a color image and Kalman filter techniques to generate a smooth estimate of the local road position. The algorithm uses two different clothoid segments, fuses saturation and color edge information and is able to cope with complex lighting conditions. Extensive tests have shown, that - with the proposed algorithm - our robot car MuCAR-3 is able to autonomously drive on significantly more dirt roads and forest tracks than before. The algorithm performs in real time. We currently are working on a procedure to evaluate the tracking results with respect to ground truth data of a test track gained from DGPS measures.

VII. Acknowledgements

The authors gratefully acknowledge funding by the Federal Office of Defense Technology and Procurement (BWB).

References

[1] V. Kastrinaki, M. Zervakis, and K. Kalaitzakis, "A Survey of video processing techniques for traffic applications," *Image and Vision Computing*, vol. 21, pp. 359–381, 2003.

[2] M. Bertozzi and A. Broggi, "GOLD: a parallel real-time stereo vision system for generic obstacle and lane detection," *IEEE Transactions on Image Processing*, vol. 7, pp. 62–81, 1998.

[3] D. Pomerleau, "RALPH: Rapidly Adapting Lateral Position Handler," *Proceedings of the International Conference on Intelligent Autonomous Systems*, pp. 505–511, September 1995.

[4] J. Crisman and C. Thorpe, "SCARF: A Color Vision System that Tracks Roads and Intersections," *IEEE Transactions on Robotics and Automation*, vol. 9, pp. 49–58, 1993.

[5] K. Kluge and C. Thorpe, "The yarf system for vision-based road following," *Mathematical and Computer Modelling*, vol. 22, pp. 213–233, 1995.

[6] K. Kluge, C. Kreucher, and S. Lakshmanan, "Tracking Lane and Pavement Edges Using Deformable Templates," *Proceedings of the SPIE Enhanced and Synthetic Vision*, vol. 3354, pp. 167–176, 1998.

[7] R. Gregor, M. Lützeler, M. Pellkofer, K. Siedersberger, and E. Dickmanns, "EMS-Vision: A Perceptual System for Autonomous Vehicles," in *Procs. IEEE Intelligent Vehicles Symposium 2000*, Detroit, USA, Oct. 2000, pp. 52–57.

[8] M. Luetzeler and S. Baten, "Road recognition for a tracked vehicle," *In Procs. SPIE Conf. on Enhanced and Synthetic Vision, Aero Sense*, vol. 4023, 2000.

[9] M. Isard and A. Blake, "CONDENSATION-Conditional Density Propagation for Visual Tracking," *IEEE International Journal of Computer Vision*, vol. 29, pp. 5–28, 1998.

[10] B. Southall and C. Taylor, "Stochastic road shape estimation," *ICCV*, vol. 1, pp. 205–212, 2001.

[11] N. Apostoloff and A. Zelinsky, "Robust vision based lane tracking using multiple cues and particle filtering," *IEEE Intelligent Vehicles Symposium*, pp. 558–563, 2003.

[12] P. Smuda, R. Schweiger, H. Neumann, and W. Ritter, "Multiple Cue Data Fusion with Particle Filters for Road Course Detection in Vision Systems," *IEEE Intelligent Vehicles Symposium*, pp. 400 – 405, 2006.

[13] U. Franke, H. Loose, and C. Knppel, "Lane Recognition on Country Roads," *IEEE Intelligent Vehicles Symposium*, pp. 99–104, 2007.

[14] M. Serfling, R. Schweiger, and W. Ritter, "Road course estimation in a night vision application using a digital map, a camera sensor and a prototypical imaging radar system," *IEEE Intelligent Vehicles Symposium*, pp. 810–815, 2008.

[15] R. Danescu, S. Nedevschi, M.-M. Meinecke, and T.-B. To, "A stereovision-based probabilistic lane tracker for difficult road scenarios," *In Procceedings of IEEE Intelligent Vehicles Symposium*, pp. 536–541, 2008.

[16] H. Loose, U. Franke, and C. Stiller, "Kalman particle filter for lane recognition on rural roads," *IEEE Intelligent Vehicles Symposium*, pp. 60–65, 2009.

[17] A. Mueller, M. Manz, M. Himmelsbach, and H.-J. Wuensche, "A model-based object following system," *IEEE Intelligent Vehicles Symposium*, 2009.

[18] E. D. Dickmanns, *Dynamic Vision for Perception and Control of Motion*. London: Springer Verlag, 2007.

[19] M. Manz, M. Himmelsbach, T. Luettel, and H.-J. Wuensche, "Fusing lidar and vision for autonomous dirt road following," *To appear in 21. Fachgespraech Autonome Mobile Systeme*, 2009.

[20] E. D. Dickmanns and A. Zapp, "A curvature-based scheme for improved road vehicle guidance by computer vision," *Proceedings of SPIE Conference on Mobile Robots*, pp. 161–168, 1986.